

# Thymidine Kinase Gene Delivery Using Curcumin Loaded Peptide Micelles as a Combination Therapy for Glioblastoma

Jin Hyeong Park · Jaesik Han · Minhyung Lee

Received: 22 May 2014 / Accepted: 15 August 2014 / Published online: 27 August 2014  
© Springer Science+Business Media New York 2014

## ABSTRACT

**Purpose** The effect of the combination therapy of curcumin and the herpes simplex virus thymidine kinase (HSVtk) gene using R7L10 as a carrier was evaluated in a glioblastoma animal model.

**Methods** Curcumin was loaded into the cores of R7L10 peptide micelles using an oil-in-water emulsion/solvent evaporation method to generate curcumin loaded R7L10 micelles (R7L10-Cur), which were used as a carrier to deliver the HSVtk gene. The plasmid DNA (pDNA)/R7L10-Cur complex was confirmed by gel retardation, heparin competition, and dynamic light scattering analyses. Transfection efficiency and cytotoxicity were measured using luciferase, MTT, and TUNEL assays. Intracellular delivery of curcumin was determined by fluorescence and absorbance. In the glioblastoma animal model, the effects of the intratumoral delivery of curcumin and the HSVtk gene were evaluated according to tumor size, immunohistochemistry, and TUNEL assays.

**Results** R7L10-Cur delivered pDNA into the cells more efficiently than PLL and R7L10. In addition, R7L10-Cur delivered curcumin into the cells more efficiently than curcumin alone. The pHSVtk/R7L10-Cur complex induced cell death efficiently both *in vitro* and *in vivo*. Likewise, the combination of curcumin and the HSVtk gene using the pHSVtk/R7L10-Cur complex reduced tumor size more efficiently than the pHSVtk/PEI and pHSVtk/R7L10 complexes in a glioblastoma animal model.

**Conclusion** R7L10 is an efficient carrier for delivery of curcumin and the HSVtk gene, which may be a useful combination therapy for glioblastoma.

**KEY WORDS** combination therapy · curcumin · gene therapy · glioblastoma · peptide micelles

## INTRODUCTION

Glioblastoma multiforme (GBM) is the most malignant type of brain tumor in humans. The current treatment options for GBM consist of surgery, radiation therapy, and chemotherapy. The core region of GBM tumors is hypoxic, which induces vascular proliferation, necrosis, and aggressive invasion into the surrounding tissues. Due to this capacity for aggressive invasion, complete resection of GBM is impossible, meaning that radiotherapy or chemotherapy is needed after surgery to further treat GBM. Although progress has been made in developing treatments for GBM, it is nevertheless associated with a poor prognosis, with a median life span of only a few months [1–4]. In addition, the existing therapies for GBM that are effective as initial treatments are associated with a wide range of undesirable side effects. Taken together, the current limitations of GBM treatments strongly support the need for development of new therapeutic options.

Gene therapy with the herpes simplex virus thymidine kinase (HSVtk) gene and the pro-drug ganciclovir (GCV) has been investigated as an alternative for the treatment of GBM [5, 6]. Transfection of cancer cells with the HSVtk gene results in expression of HSVtk, which transforms non-toxic GCV into toxic phosphorylated GCV. In turn, toxic phosphorylated GCV inhibits DNA synthesis and induces apoptosis in dividing cells. In addition, toxic GCV can transfer to neighboring cancer cells through gap junctions to induce cell death [7] through the so called “bystander effect.” Due to these characteristics, HSVtk gene therapy has been proposed as a useful anti-cancer strategy.

To increase the effectiveness of gene therapy, combinations of specific genes and drugs have been studied as new treatment strategies for GBM. For example, temozolomide (TMZ) was studied as a combination treatment for GBM with the

J. H. Park · J. Han · M. Lee (✉)  
BK21 Plus Future Biopharmaceutical Human Resources Training and  
Research Team, Department of Bioengineering, College of Engineering  
Hanyang University, Seoul 133-791, Republic of Korea  
e-mail: minhyung@hanyang.ac.kr

HSVtk gene [8, 9]. In another study, O<sub>6</sub>-methylguanine-DNA methyltransferase (MGMT) siRNA was combined with TMZ [10]. Similarly, the VEGF siRNA was combined with docetaxel (DTX) for the treatment of glioblastoma [11].

In the current study, we evaluated the combination therapy of curcumin and the HSVtk gene. Curcumin has been used as an anti-inflammatory and antioxidant drug [12], and was recently reported to have anti-proliferative effects in various cancers, including glioblastoma [13–15]. However, curcumin is very hydrophobic and thus is poorly soluble in water. Therefore, an effective solubilizer is required to deliver curcumin into cells [16, 17].

We previously studied the amphiphilic peptide R7L10 as a carrier for both drugs and for gene delivery [18]. The R7L10 peptide is composed of a 7-arginine stretch and a 10-leucine stretch, and forms a micelle structure in aqueous solution that can be loaded with hydrophobic drugs. We showed that curcumin could be loaded into R7L10 micelles, and evaluated the resulting curcumin loaded R7L10 micelles (R7L10-Cur) as a drug and gene carrier for the treatment of acute lung injury [18]. The results of this study showed that R7L10-Cur has a high drug and gene delivery efficiency in lung cells *in vitro* and *in vivo* [18].

In the current study, R7L10 was used as a carrier of curcumin and the HSVtk gene for the treatment of glioblastoma. The plasmid DNA (pDNA)/R7L10-Cur complex was characterized by various methods, after which drug and gene delivery efficiencies of the pDNA/R7L10-Cur complex were evaluated *in vitro* with C6 glioblastoma cells. Lastly, the anti-cancer effect of the curcumin and HSVtk gene combination therapy was evaluated in a glioblastoma mouse model.

## MATERIAL AND METHODS

### Materials

Curcumin, polyethylenimine (PEI, 25 kDa), poly-L-lysine (PLL), heparin, and 3-[4,5-dimethylthiazol-2-yl]-2,5-diphenyltetrazoliumbromide (MTT) were purchased from Sigma-Aldrich (St. Louis, MO). The bicinchoninic acid (BCA) assay kit was purchased from Pierce (Thermo Fisher Scientific, Waltham, MA). The luciferase assay kit, reporter lysis buffer, terminal deoxynucleotide transferase-mediated dUTP nick-end labeling (TUNEL) assay kit and pEmpty (pSI) were purchased from Promega (Madison, WI). An immunohistochemistry accessory kit was purchased from Bethyl Laboratories (Montgomery, TX). C6 cell lines were obtained from the Korean Cell Line Bank (Seoul, Korea). Fetal bovine serum (FBS) and Dulbecco's modified Eagle's medium (DMEM) were purchased from GIBCO (Gaithersburg, MD). Ganciclovir was purchased from InvivoGen (San Diego, CA).

### Preparation of Curcumin Loaded R7L10

R7L10 was chemically synthesized by Peptron Co (Daejeon, Korea). R7L10-Cur was prepared in R7L10/curcumin weight ratios of 1:0.2, 0.4, and 0.6 (molar ratios of 1:1.2, 2.4, and 3.6). Curcumin was loaded into R7L10 peptide micelles using an oil-in-water (O/W) emulsion/solvent evaporation method as described previously [18]. Briefly, R7L10 and curcumin were dissolved in distilled water and ethanol, respectively, and the two solutions were mixed slowly, dispersed in distilled water with sonication for 90 s, and lyophilized using a freeze-dryer. Lyophilized R7L10-curcumin was readily resuspended in distilled water.

### Preparation of pDNAs

The pDNA used in this study consisted of p $\beta$ -Luc and pHSVtk. p $\beta$ -Luc was constructed by insertion of the luciferase cDNA isolated from pGL3-promoter (Promega, Madison, WI) into the *HinDIII* and *XbaI* sites of p $\beta$ . The HSVtk expression plasmid, pHSVtk (pEpo-NI2-SV-HSVtk), was constructed previously [19]. pDNAs were transformed in *Escherichia Coli* DH5 $\alpha$ , amplified in Terrific Broth media at 37°C overnight, and purified using a Maxi plasmid purification kit (Qiagen, Valencia, CA).

### Gel Retardation Assay

A fixed amount of pDNA (1  $\mu$ g) was mixed with increasing amounts of R7L10 or R7L10-Cur. The resulting mixtures were incubated for 30 min at room temperature and analyzed on 1% agarose gels by electrophoresis.

### Heparin Competition Assay

pDNA/carrier complexes were prepared at their optimum conditions for transfection. The pDNA/R7L10 and pDNA/R7L10-Cur complexes were prepared at a 1:5 weight ratio based on the transfection assay results. Likewise, pDNA/PLL complexes were prepared at a 1:2 weight ratio and pDNA/PEI complexes were prepared at a 5:1 N/P ratio based on the results of two previous studies [20, 21]. The resulting pDNA/carrier complexes were incubated for 30 min at room temperature, after which increasing amounts of heparin were added to the complexes and incubated for 30 min at room temperature. Finally, the complexes were electrophoresed on 1% agarose gels.

### Measurement of Zeta-Potential and Complex Size

The pDNA/carrier complexes were prepared at their optimum ratio for transfection and incubated for 30 min at room temperature. The particle sizes and zeta potentials were then

determined using a Zetasizer Nano ZS system (Malvern Instruments, Malvern, UK).

### Cell Culture and Transfection

C6 rat glioblastoma and human embryonic kidney 293 (HEK293) cells were maintained in DMEM supplemented with 10% FBS. Next, the cells were cultured at 37°C in a 5% CO<sub>2</sub> incubator. C6 cells were seeded at a density of  $1 \times 10^5$  cells/well in 12-well plates 24 h before transfection. For optimization of transfection conditions, the p $\beta$ -Luc/R7L10 and p $\beta$ -Luc/R7L10-Cur complexes were prepared at various weight ratios. For comparison of R7L10-Cur with other carriers, p $\beta$ -Luc/R7L10 and p $\beta$ -Luc/R7L10-Cur complexes were prepared at an optimized ratio. The p $\beta$ -Luc/PLL and p $\beta$ -Luc/PEI complexes were prepared at 1:2 and 1:1 weight ratios based on the results of two previous studies [20, 21]. Next, the prepared complexes were added to cells and incubated for an additional 24 h at 37°C in a 5% CO<sub>2</sub> incubator. After incubation, transfection efficiency was analyzed by luciferase assay

### Luciferase Assay

After transfection, cells were washed twice with 0.5 ml of PBS. Next, 120  $\mu$ L of the reporter lysis buffer was added to each well and incubated for 15 min at room temperature. The cell extracts were harvested, transferred to microcentrifuge tubes, and vortexed for 15 s. The resulting lysate was then centrifuged at 13,000 rpm for 3 min, after which the supernatants were transferred to new microcentrifuge tubes. The protein concentrations of the extracts were measured using a BCA assay kit. Luciferase activity was measured using a 96-well plate luminometer (Berthold Detection System GmbH, Pforzheim, Germany). Final luciferase activities were reported as relative light units (RLU)/mg total protein.

### Cytotoxicity Assay

MTT assays were performed to evaluate the cytotoxicity of the different complexes. The pDNA/carrier complexes were added to C6 or HEK293 cells and incubated for 24 h at 37°C. After incubation, 40  $\mu$ L of 5 mg/ml MTT solution in PBS was added to each well. The cells were then incubated for an additional 4 h at 37°C. After the incubation, medium containing the MTT solution was removed and 750  $\mu$ L of DMSO was added to dissolve the formazan crystals formed by reduction of MTT in living cells. The absorbance at 570 nm was measured by a microplate reader, and cell viability (%) was calculated according to the following equation:

$$\text{Cell viability (\%)} = (\text{OD}_{570}(\text{sample})/\text{OD}_{570}(\text{control})) \times 100.$$

### Intracellular Curcumin Delivery Assay

C6 cells were seeded at a density of  $1 \times 10^5$  cells/well in 12-well plates and incubated for 24 h at 37°C before transfection. C6 cells were then treated with either R7L10-Cur, a simple mixture of R7L10 and curcumin, or curcumin alone and then incubated for 24 h at 37°C. After treatment, cell extracts were prepared with reporter lysis buffer as described above. Absorbance at 450 nm was measured using a SpectraMax plate reader (Molecular Devices, Sunnyvale, CA), and the fluorescence of each sample was measured with an excitation and emission of 485 and 538 nm, respectively (Molecular Devices, Sunnyvale, CA).

### In vitro TUNEL Assay

C6 cells were seeded at a density of  $1 \times 10^5$  cells/well in chamber slides and incubated for 24 h at 37°C before transfection. The complexes were then added to C6 cells and incubated for 24 h at 37°C in medium containing 10  $\mu$ g/ml GCV. At the end of the transfection experiment, cells were washed twice with 0.5 ml of PBS. The TUNEL assay was performed according to the manufacturer's instructions.

### In vivo Experiments in the Subcutaneous Glioblastoma Xenograft Mouse Model

All *in vivo* experiments were performed according to the guidelines of the Hanyang University Animal Research Committee, who approved the study protocol. Five weeks old male Balb/c nude mice were anesthetized and inoculated with  $1 \times 10^5$  C6 cells into the dorsal flank of each mouse to establish subcutaneous tumors. After the tumor reached a diameter of 4–6 mm, mice were randomly allocated and injected with pDNA/carrier complexes, with each group consisting of 10 mice. All complexes were prepared at their respective optimized ratios in a total volume of 50  $\mu$ L saline, with the amount of pDNA fixed at 15  $\mu$ g/head. The complexes were injected intratumorally 3 times at an interval of 3 days between injections. After the first complex injection, GCV (25 mg/kg) was injected intraperitoneally daily for 14 days. Tumor volume was measured with calipers every 3 days for 21 days. Finally, tumor volume was calculated using the formula: length (mm)  $\times$  width (mm)<sup>2</sup>  $\times$  0.5.

### Immunohistochemistry and TUNEL Assay

Four animals from each group were sacrificed 3 days after injections were completed for immunohistochemistry and TUNEL assay. The tumors were then harvested, fixed with a 4% paraformaldehyde solution, embedded in paraffin, and finally cut into 5- $\mu$ m thick sections using a microtome. HSVtk

immunohistochemistry and TUNEL assays were performed according to the manufacturer's instructions.

### Statistical Analysis

Statistical analyses were conducted using ANOVA followed by the Newman-Keuls test. All data are expressed as the average  $\pm$  SEM, with  $P < 0.05$  considered to be statistically significant.

## RESULTS

### Characterization of pDNA/R7L10 and pDNA/R7L10-Cur Complexes

Gel retardation assays were performed to confirm the formation of a complex between pDNA and R7L10-Cur. A fixed amount of pDNA was mixed with increasing amounts of R7L10 and R7L10-Cur. In gel retardation assays, pDNA was completely retarded with R7L10 or R7L10-Cur at a 1:1.5 weight ratio (pDNA/carrier), suggesting the formation of a complex between pDNA and R7L10 or R7L10-Cur (Fig. 1a). Next, heparin competition assays were performed to evaluate the stability of the complexes. The heparin competition assay showed that the pDNA/R7L10 and pDNA/R7L10-Cur complexes did not release pDNA even up to 50  $\mu$ g of heparin (50 fold excess of the amount of pDNA) (Fig. 1b). However, PLL began to release pDNA in the presence of 5  $\mu$ g of heparin from the pDNA/PLL complexes and released pDNA completely with 10  $\mu$ g of heparin. Similarly, the pDNA/PEI complex released pDNA more easily than the pDNA/R7L10 or pDNA/R7L10-Cur complex, suggesting that R7L10 and R7L10-Cur formed stable complexes with pDNA.

The particle sizes of the pDNA/carrier complexes were measured by dynamic light scattering (Table I). The average mean diameter of the pDNA/R7L10 complex was approximately 194 nm, while that of pDNA/R7L10-Cur complex was approximately 211 nm. The particle size of pDNA/R7L10-Cur was slightly larger than that of the pDNA/PLL and pDNA/PEI complexes. The surface charges of the pDNA/R7L10 and pDNA/R7L10-Cur complexes were 37 and 52 mV, respectively (Table I).

### In vitro Transfection

To optimize the transfection conditions for R7L10, pDNA/R7L10 complexes were prepared and transfected into C6 cells at various weight ratios. The highest transfection efficiency of R7L10 was obtained at a weight ratio of 1:5 (Fig. 2a). The cytotoxicity of R7L10 was measured in C6 (Fig. 2b) and

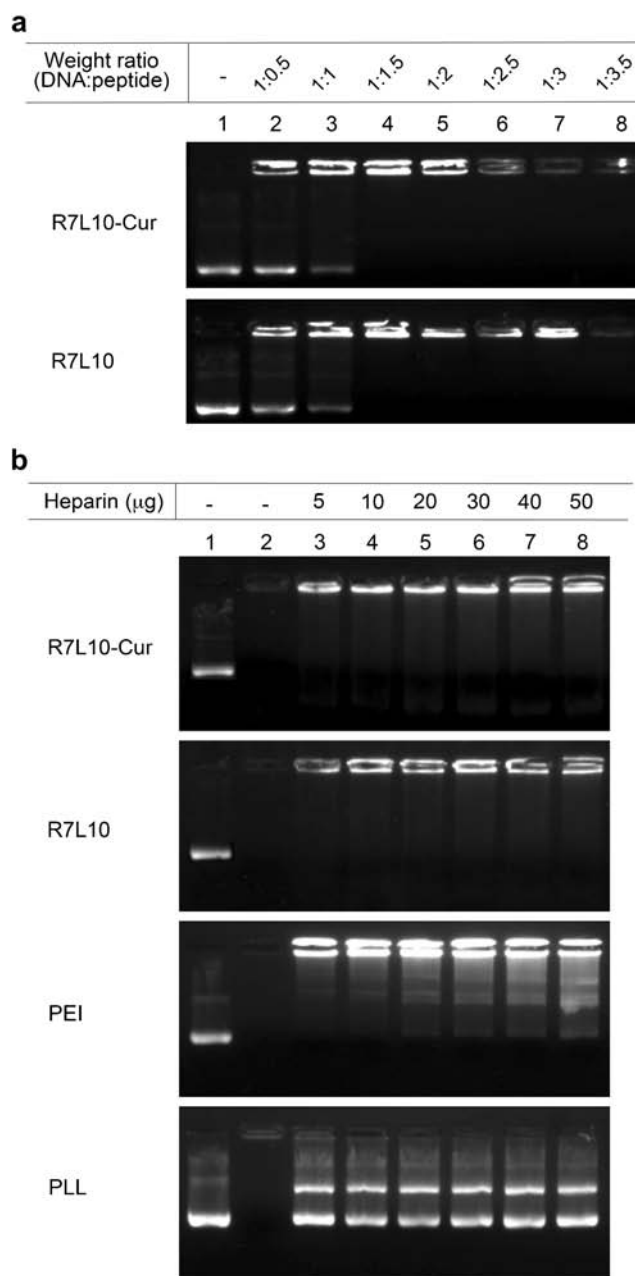


**Fig. 1** Physical characterization. **(a)** Gel retardation assay pDNAs were mixed with increasing amounts of R7L10 or R7L10-Cur. After incubation for 30 min at room temperature the samples were analyzed on a 1% agarose gel. **(b)** Heparin competition assay pDNA/carrier complexes were prepared at their optimal transfection ratios and increasing amounts of heparin were added to the complexes. After incubation for 30 min at room temperature the complexes were analyzed on a 1% agarose gel

HEK293 cells (Fig. 2c). pDNA/R7L10 complexes were prepared at a 1:5 weight ratio, and pDNA/PEI and pDNA/PLL complexes were prepared at 1:1 and 1:2 weight ratios, respectively, according to previous research [20, 21]. The results of the MTT assays showed that R7L10-treated cells had a higher viability than that of PEI and PLL, suggesting that R7L10 was less cytotoxic (Fig. 2b and c).

**Table 1** Particle size and Zeta potential

Group	Size (d, nm)	Zeta potential (mV)
pDNA/PEI	139.21 ± 17.63	54.27 ± 2.22
pDNA/PLL	117.41 ± 19.98	23.54 ± 7.21
pDNA/R7L10	194.03 ± 20.41	37.89 ± 5.47
pDNA/R7L10-Cur	211.72 ± 15.28	52.08 ± 4.08

pDNA/carrier complexes were prepared at their optimum ratios for transfection. The size and zeta potentials are presented as the mean ± standard deviation

R7L10-Cur may have had a different transfection efficiency compared to R7L10, since loading curcumin into the cores of the R7L10 micelles may have increased their stability. To evaluate the transfection efficiency of R7L10-Cur, curcumin was loaded into the R7L10 micelle at weight ratios of 1:0.2, 1:0.4, and 1:0.6 (R7L10:curcumin). The transfection efficiencies of different R7L10-Cur were optimized in terms of the weight ratio between pDNA and R7L10-Cur. The transfection assays showed that R7L10-Cur (R7L10:curcumin = 1:0.2) and R7L10-Cur (R7L10:curcumin = 1:0.6) exhibited the highest transfection efficiency at a weight ratio of 1:5 (pDNA:R7L10-Cur) (Fig. 3a). Likewise, R7L10-Cur (R7L10:curcumin = 1:0.4) showed the highest transfection efficiency at a weight ratio of 1:7 (Fig. 3a). Considering that higher doses of curcumin may be associated with a better therapeutic effect, R7L10-Cur at a 1:0.6 R7L10:curcumin weight ratio was used for subsequent experiments. In addition, the transfection efficiency of R7L10-Cur was compared with that of R7L10, PEI, and PLL. These results showed that R7L10-Cur exhibited increased transfection efficiency compared with R7L10 (Fig. 3b). Specifically, the transfection efficiency of R7L10-Cur was higher than PLL but lower than PEI (Fig. 3b). The lower transfection efficiency of R7L10-Cur compared to PEI may represent a disadvantage for its capacity as a gene carrier; however, this is mitigated by the fact that R7L10-Cur delivers both curcumin as well as a therapeutic gene, whereas PEI delivers only a therapeutic gene.

Therefore, R7L10-Cur may be more suitable as a combination therapy consisting of curcumin and the HSVtk gene compared with PEI.

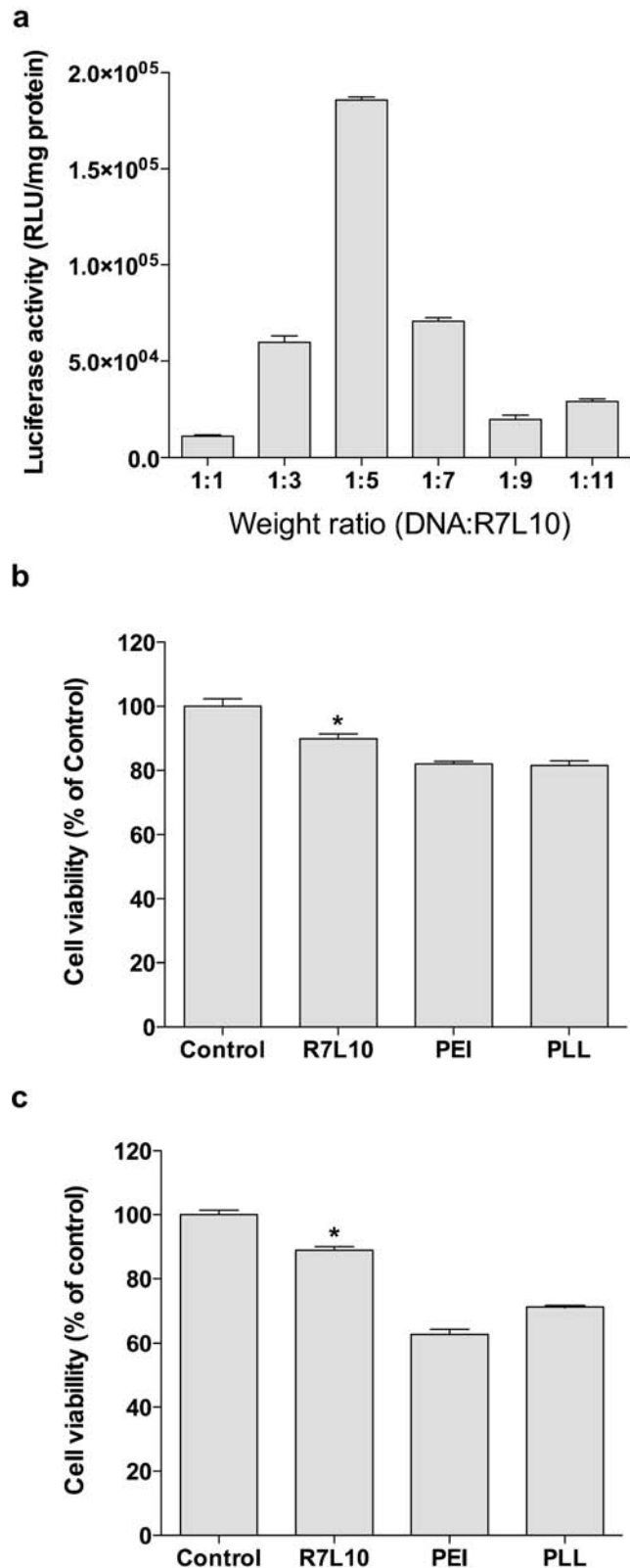


**Fig. 2** Transfection efficiency and cytotoxicity of R7L10. **(a)** Transfection efficiency pβ-Luc/R7L10 complexes were prepared at various weight ratios and transfected into C6 cells. After 24 h, gene expression was measured by luciferase assay. Luciferase activities are presented as the mean ± standard error of quadruplicate experiments. **(b)** Cytotoxicity in C6 glioblastoma cells pDNA/R7L10, pDNA/PLL, and pDNA/PEI complexes were prepared at their optimum ratios for transfection. The complexes were then transfected into C6 cells, and after 24 h their cytotoxicities were measured by MTT assay. Cell viability data is presented as the mean ± standard error of quadruplicate experiments. \* $P < 0.05$  as compared with control and other carriers. **(c)** Cytotoxicity in HEK293 cells. The complexes were then transfected into the HEK293 cells, and after 24 h their cytotoxicities were measured by MTT assay. Cell viability data is presented as the mean ± standard error of quadruplicate experiments. \* $P < 0.05$  as compared with control and other carriers.



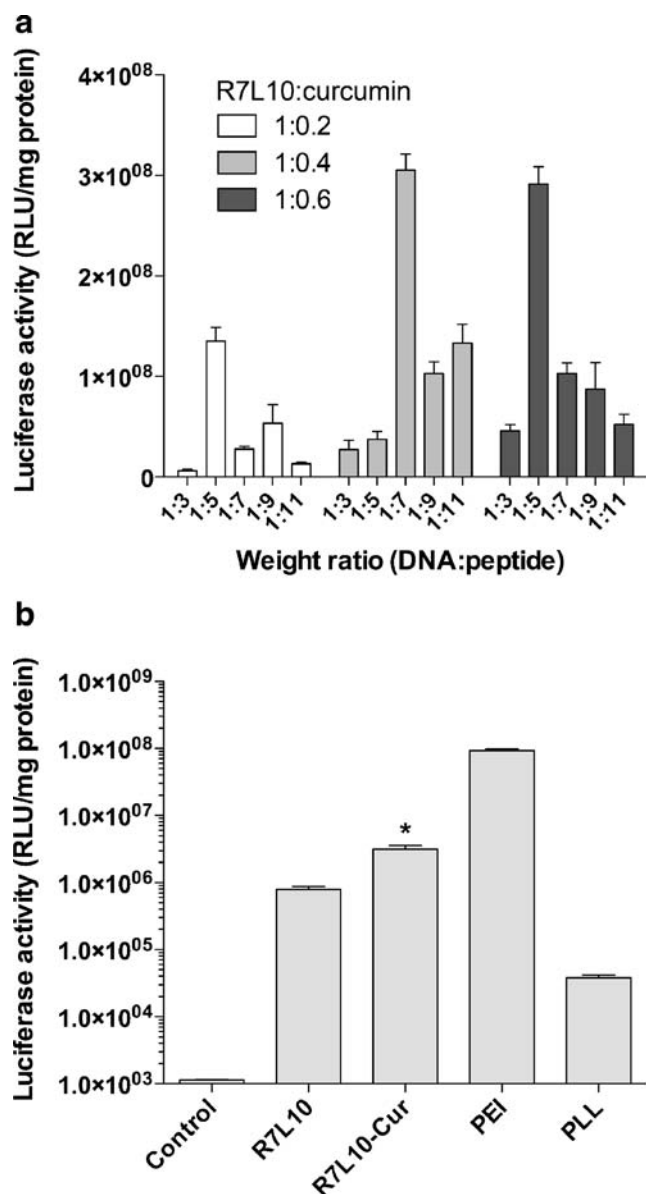


**Fig. 3** Transfection efficiency of R7L10-Cur. **(a)** Transfection efficiency of R7L10-Cur at various weight ratios. R7L10-Cur was prepared at weight R7L10:curcumin ratios of 1:0.2, 1:0.4 and 1:0.6. The p $\beta$ -Luc/R7L10-Cur complexes were prepared at various weight pDNA:R7L10-Cur ratios and transfected into C6 cells. **(b)** Comparison of R7L10-Cur with other carriers. pDNA/R7L10, pDNA/R7L10-Cur, pDNA/PLL, and pDNA/PEI complexes were prepared at their optimum ratios and transfected into C6 cells. After 24 h, transfection efficiencies were measured by luciferase assay. Luciferase activities are presented as the mean  $\pm$  standard error of quadruplicate experiments. \* $P < 0.01$  as compared with control and other carriers

### Curcumin Delivery Efficiency of R7L10-Cur

C6 cells were incubated with R7L10-Cur, curcumin only, or a simple mixture of curcumin and R7L10, and the efficiency of curcumin delivery into cells was measured by absorbance and fluorescence. The absorbance results showed that R7L10-Cur had higher

curcumin delivery efficiency of curcumin compared with curcumin alone or a simple mixture of curcumin and R7L10 (Fig. 4a). These results were confirmed by fluorescence measurements (Fig. 4b). Therefore, loading curcumin into micelles increased the efficiency of curcumin delivery.

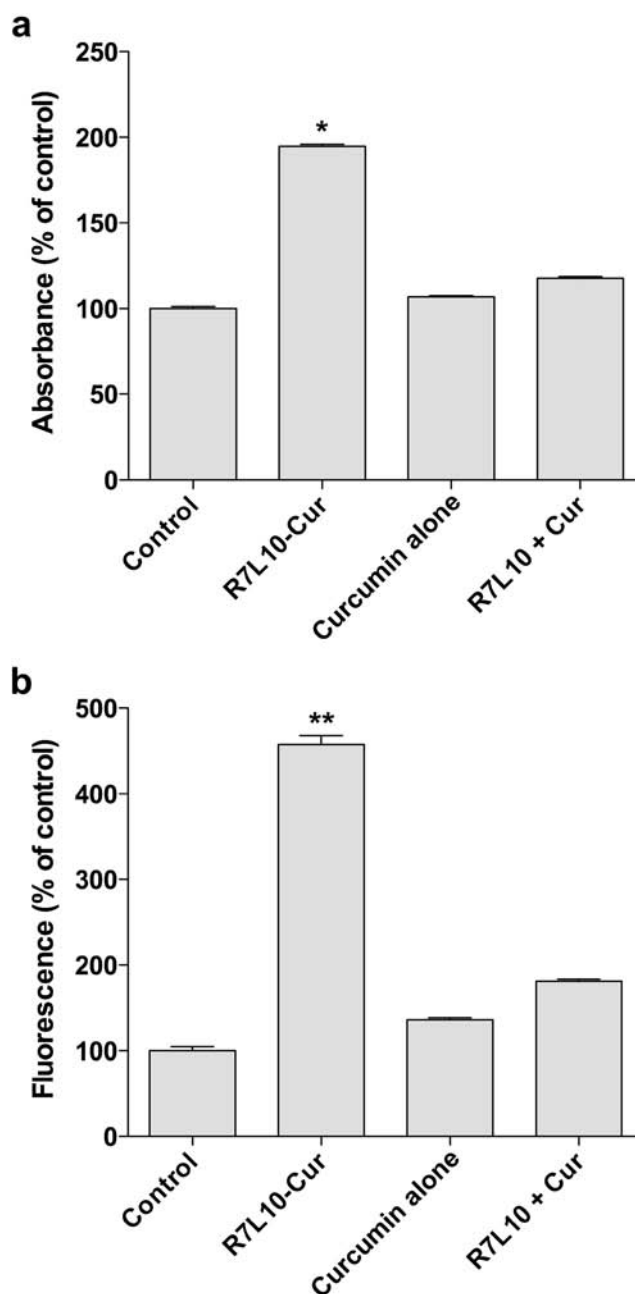


**Fig. 4** Curcumin delivery efficiency of R7L10-Cur. R7L10-Cur, curcumin only, and a simple mixture of curcumin and R7L10 were added to C6 cells. After 24 h, the intracellular concentration of curcumin was measured by **(a)** absorbance and **(b)** fluorescence. Data are presented as the mean  $\pm$  standard error of quadruplicate experiments. \*, \*\* $P < 0.01$  as compared with all other groups

### In vitro Anti-Tumor Effect of the Combination of Curcumin and the HSVtk Gene

The pHSVtk/PEI, pHSVtk/R7L10, and pHSVtk-R7L10-Cur complexes were prepared and transfected into C6 cells. Next, cells were incubated with media containing GCV, and MTT assays were performed to measure the anti-cancer effects of the complexes. The pHSVtk/R7L10 complex exhibited a weaker anti-cancer effect than that of the pHSVtk/PEI complex, suggesting that the pHSVtk/PEI complex had a higher gene delivery efficiency than the pHSVtk/R7L10 complex (Fig. 5a). This result was consistent with the transfection assay

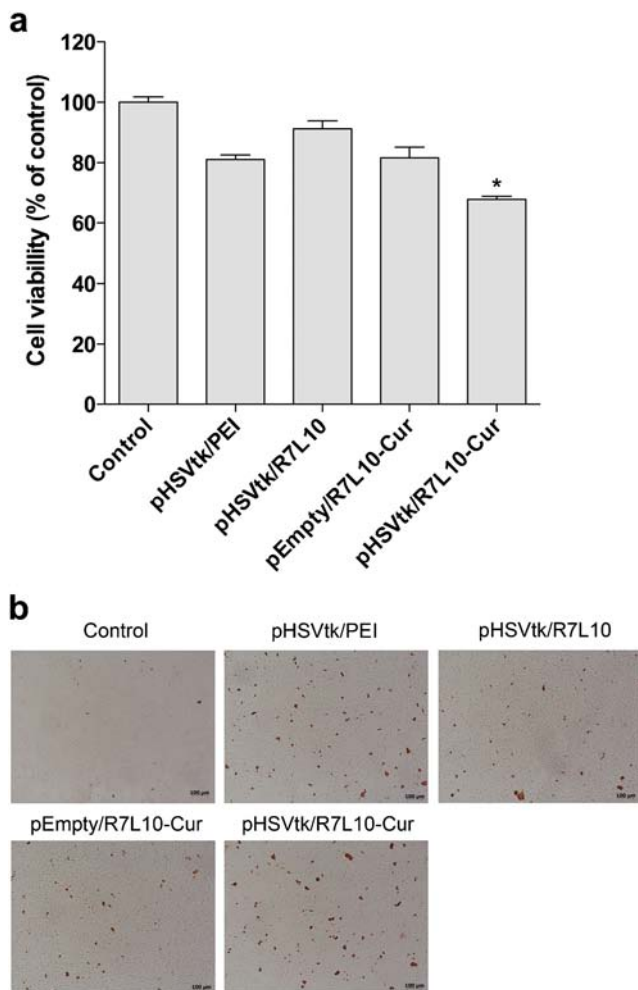


**Fig. 5** Cytotoxicity of the TK/R7L10-Cur complex. **(a)** MTT assay. The pHSVtk/R7L10-Cur, pHSVtk/R7L10, pHSVtk/PEI, and pEmpty/R7L10-Cur complexes were prepared at their optimum ratios and transfected into C6 cells incubated with GCV (10  $\mu$ g/ml). After 24 h, the cytotoxicities of the complexes were measured by MTT assay. Cell viability data is presented as the mean  $\pm$  standard error of quadruplicate experiments. \* $P < 0.01$  as compared with control and all other complexes. **(b)** Apoptosis induced by the pHSVtk/R7L10-Cur complex. pHSVtk/carrier complexes were prepared at their optimum ratios and transfected into C6 cells incubated with GCV (10  $\mu$ g/ml). After 24 h, the extent of apoptosis was measured by TUNEL assay. Apoptotic cells are stained in brown, 100 $\times$  magnification

findings with the luciferase gene. However, the pHSVtk/R7L10-Cur complex had a higher anti-cancer effect than the pHSVtk/PEI and pEmpty/R7L10-Cur complex, suggesting a combination effect of curcumin and the HSVtk gene (Fig. 5a).

The anti-cancer effects of the pHSVtk/R7L10-Cur complexes were due in part to apoptosis based on the TUNEL assay. Specifically, the pHSVtk/R7L10-Cur complex induced apoptosis in cells more efficiently than any of the other complexes evaluated (Fig. 5b).

### In vivo Anti-Tumor Effect of Combined Curcumin and HSVtk Gene Delivery

First, the anti-tumor effect of pHSVtk was evaluated in the glioblastoma animal models. For the *in vivo* study, the pEmpty/R7L10-Cur and pHSVtk/R7L10-Cur complexes were prepared and injected intratumorally into glioblastoma xenograft animal models, and tumor volumes were measured every 3 days. The results confirmed that the pHSVtk/R7L10-Cur complex inhibited the tumor growth more effectively than pEmpty/R7L10-Cur complex, suggesting the anti-tumor effect of pHSVtk (Fig. 6).

To evaluate the anti-tumor effect of the combined delivery of curcumin and the HSVtk gene, pHSVtk was delivered using R7L10-Cur, R7L10, and PEI as carriers. The pHSVtk/PEI, pHSVtk/R7L10 and pHSVtk/R7L10-Cur complexes were prepared at their optimized ratios and injected intratumorally into glioblastoma xenograft animal models. The results showed that the pHSVtk/R7L10-Cur complexes suppressed tumor growth more effectively than the pHSVtk/R7L10 and pHSVtk/PEI complexes (Fig. 7a). Similar to the *in vitro* study, the HSVtk/PEI complex had higher anti-tumor effect than the HSVtk/R7L10 complex (Fig. 7a). However, the combination of curcumin and HSVtk using the pHSVtk/R7L10-Cur

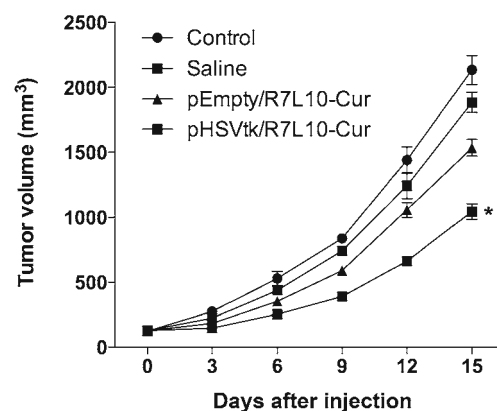


**Fig. 6** Anti-cancer effect of pHSVtk in a subcutaneous glioblastoma model. pDNA/carrier complexes were prepared at their optimum ratios and injected intratumorally three times at an interval of 3 days. Tumor volume was calculated using the formula length (mm)  $\times$  width (mm)<sup>2</sup>  $\times$  0.5. Data are presented as the mean  $\pm$  standard error. \* $P < 0.05$  compared with all other groups

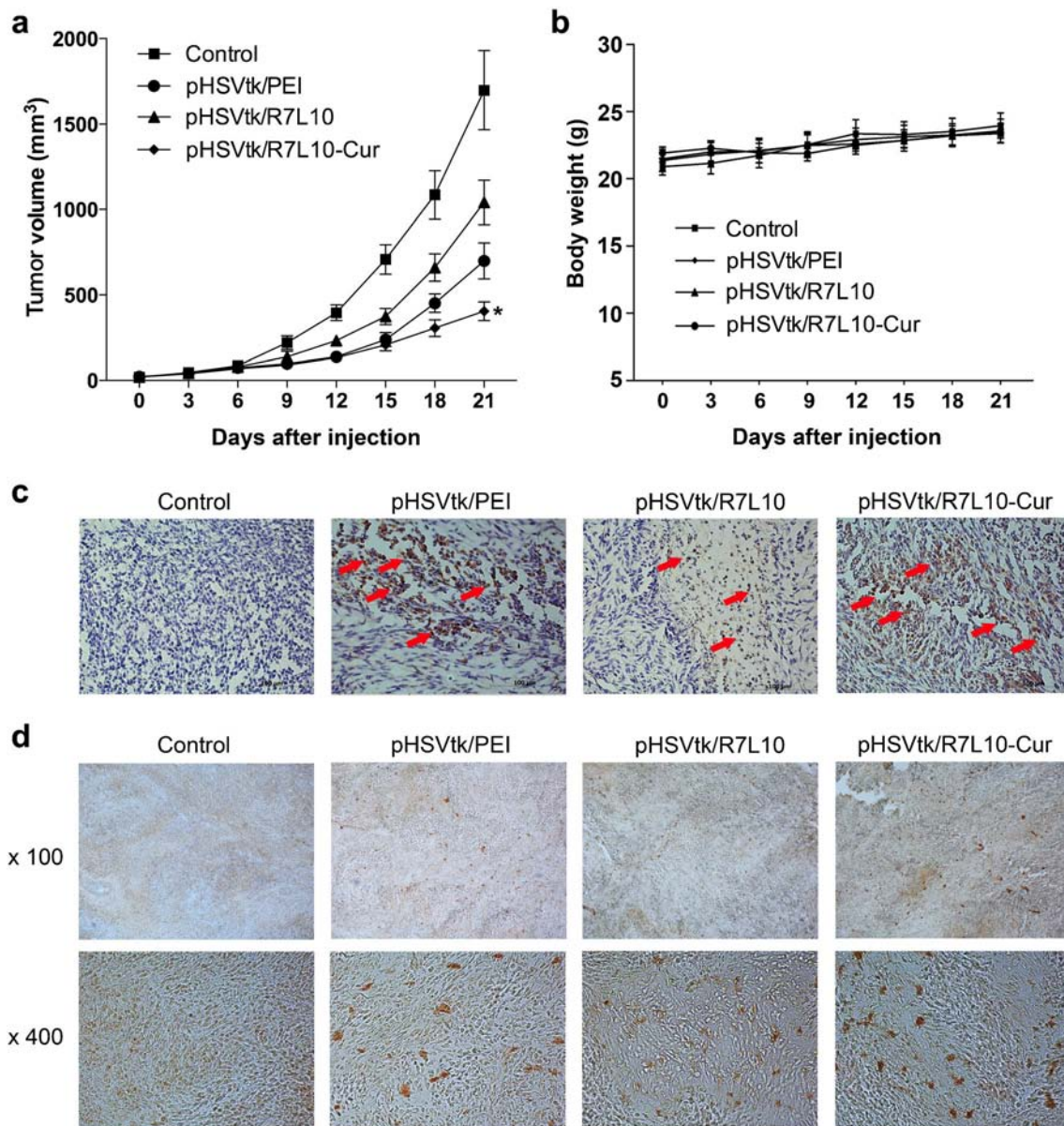


**Fig. 7** Anti-cancer effect of pHSVtk/R7L10-Cur complex in a subcutaneous glioblastoma model. **(a)** Tumor volume. pDNA/carrier complexes were prepared at their optimum ratios and injected intratumorally three times at an interval of 3 days. Tumor volume was calculated using the formula length (mm)  $\times$  width (mm)<sup>2</sup>  $\times$  0.5. Data are presented as the mean  $\pm$  standard error. \* $P < 0.05$  compared with all other groups. **(b)** Body weights. **(c)** HSVtk immunohistochemistry and **(d)** TUNEL assay. Tumors were harvested 3 days after the last injection, processed, sectioned, and subjected to immunohistochemical and TUNEL assays. HSVtk positive cells and apoptotic cells are stained in brown. Immunohistochemistry,  $\times 400$  magnification; TUNEL assay,  $\times 100$  and  $\times 400$  magnification

complex resulted in an increased anti-tumor effect, with the pHSVtk/R7L10-Cur complex showing a higher anti-cancer effect than the pHSVtk/PEI complex. The body weights of the groups were not significantly different from one another. This suggests that the complexes did not induce significant systemic toxicity (Fig. 7b).

Immunohistochemistry results showed that the HSVtk gene was expressed in the pHSVtk/PEI, pHSVtk/R7L10, and pHSVtk/R7L10-Cur groups, but not in the control group (Fig. 7c). The HSVtk/R7L10-Cur group had similar HSVtk expression as the HSVtk/PEI group. In addition, the

results of the *in vivo* TUNEL assay were similar to the *in vitro* TUNEL assay. Lastly, the HSVtk/R7L10-Cur group induced the highest number of apoptotic cells among the different treatments that were evaluated (Fig. 7d).

## DISCUSSION

Gene delivery of HSVtk with GCV has been investigated as a novel treatment strategy for glioblastoma [5, 6]. Likewise,



curcumin has been investigated as an anti-tumor agent for various tumors including glioblastoma [22, 23]. Therefore, we hypothesized that a combination therapy of curcumin and HSVtk gene delivery may increase the therapeutic effect on the treatment of glioblastoma, and evaluated the possibility of using this combination therapy both *in vitro* and *in vivo*. In support of our hypothesis, we found that the R7L10 peptide micelles were an efficient carrier of curcumin and the HSVtk gene and that the combination of curcumin and the HSVtk gene increased the therapeutic effect.

R7L10 is an efficient carrier for combined delivery of curcumin and the HSVtk gene. In aqueous solution, R7L10 forms a micelle structure that has a cationic surface and a hydrophobic core. The cationic surface of R7L10 micelles contributes to complex formation *via* electrostatic attraction. Physical characterization showed that R7L10 and R7L10-Cur formed stable complexes with pDNAs (Fig. 1). *In vitro* transfection assays showed that R7L10-Cur had a higher transfection efficiency than R7L10, which may have been due to stabilization of the micelle structure by curcumin. In addition, curcumin may serve as a hydrophobic core for the formation of the R7L10 micelles and thus facilitate R7L10 micelle formation. In this way, R7L10 micelles are likely stabilized by the presence of curcumin to allow for increased formation of stable complexes with pDNA. These results were similar to those described in previous studies [18, 24], which showed that pDNA/R7L10-Cur complexes have increased stability and transfection efficiency compared with pDNA/R7L10 complexes in lung epithelial cells [18].

The transfection efficiency of R7L10-Cur was lower than PEI (Fig. 3b). The lower luciferase expression of the pDNA/R7L10-Cur complexes may be partly due to anti-tumor effect of curcumin, since curcumin induced cell death of the transfected tumor cells (Fig. 5). In the previous study, R7L10-curcumin was evaluated as a gene carrier into the L2 lung epithelial cells, which are not tumor cells [18]. The results showed that R7L10-Cur had lower transfection efficiency than PEI in the L2 cells. This suggests that lower luciferase expression in the pDNA/R7L10-Cur transfected cells is also due to lower transfection efficiency of R7L10.

R7L10 was hypothesized to be an efficient carrier of not only pDNAs, but also curcumin. To confirm this possibility, we compared R7L10-curcumin and a simple mixture of R7L10 and curcumin in terms of their relative efficiencies for intracellular delivery of curcumin. The results of this analysis confirmed that curcumin could be loaded into the cores of the R7L10 micelles for higher delivery efficiency (Fig. 4). Indeed, the positive charge of R7L10-Cur may increase the interaction between cells and R7L10-curcumin, since the cellular membrane has a negative charge and attracts positively charged R7L10-Cur. Another advantage of R7L10 is that R7L10 is a good solubilizer of curcumin, which itself is hydrophobic and water insoluble. As shown in Fig. 4,

curcumin had to be solubilized in ethanol. In contrast, R7L10-Cur was readily soluble in water. Taken together, these results indicated that R7L10 is an excellent carrier of curcumin and the HSVtk gene.

In this study, pDNA/R7L10-Cur complex was injected intratumorally in the animal model. Intravenous injection of the pDNA/R7L10-Cur complex may be a useful application for the treatment of glioblastoma. However, there are some issues that should be addressed. First, R7L10-Cur has lower charge density than cationic polymer such as PEI. Therefore, after intravenous injection, pDNA/R7L10-Cur may be easily dissociated by the interaction with charged molecules in the blood. Second, blood-brain-barrier (BBB) may reduce the pDNA delivery efficiency greatly. Therefore, targeting ligands for brain delivery should be introduced to the peptide micelles.

The results of our study showed that the pHSVtk/R7L10 complex had a lower therapeutic effect than the pHSVtk/PEI complex (Figs. 5 and 7), whereas loading curcumin into the R7L10 micelles increased the anti-tumor effect significantly. Specifically, the pHSVtk/R7L10-Cur complex had a higher anti-cancer effect than the pHSVtk/PEI and pHSVtk/R7L10 complexes *in vitro* and *in vivo* (Figs. 5 and 7). This higher anti-cancer effect may have been due to two different properties of the pHSVtk/R7L10-Cur complex. First, the gene delivery efficiency of R7L10-Cur was approximately seven times greater than that of R7L10 (Fig. 3a). Considering that the transfection efficiency of R7L10-Cur was less than that of PEI (Fig. 3b), the higher delivery efficiency of R7L10-Cur suggested that the enhanced HSVtk gene delivery efficiency was at least partially responsible for the increased anti-cancer effects of pHSVtk/R7L10-Cur compared with pHSVtk/PEI. Secondly, the anti-cancer effects of curcumin were considered to play a role in the anti-cancer effects of pHSVtk/R7L10-Cur. Importantly, curcumin exhibited an additive effect with the HSVtk gene in the HSVtk/R7L10-Cur complex, suppressing tumor growth more effectively than the pHSVtk/PEI complex (Fig. 7).

Anti-tumor effect of curcumin may be due to down-regulation of cytokines. It was previously reported that curcumin down-regulated proinflammatory cytokines such as interleukin-1 $\alpha$  (IL-1 $\alpha$ ), IL-1 $\alpha$ , tumor necrosis factor- $\alpha$  (TNF- $\alpha$ ), and IL-6 [18, 25–27]. Proinflammatory cytokines are involved in cancer development, since they can activate oncogenic transcription factors such as nuclear factor- $\kappa$ B (NF- $\kappa$ B) and activating protein-1 (AP-1). Therefore, curcumin inhibits inflammation and cancer progression by down-regulation of proinflammatory cytokines [25–27].

In summary, R7L10-Cur exhibited a higher transfection efficiency compared with R7L10 and PLL into the C6 glioblastoma cells. In addition, R7L10 enhanced the intracellular delivery efficiency of curcumin. Together, these results suggested that R7L10 is a good carrier for combined delivery of

curcumin and the HSVtk gene. The combination therapy of curcumin and the HSVtk gene increased the therapeutic effect on the suppression of tumor growth in the xenograft glioblastoma model. Therefore, combination therapies utilizing curcumin and the HSVtk gene delivered using R7L10-Cur may be useful for the treatment of glioblastoma.

## ACKNOWLEDGMENTS AND DISCLOSURES

This work was financially supported by a grant from the National Research Foundation of Korea, funded by the Ministry of Science, ICT and Future Planning (Grant number, 2013K000257 and NRF-2013R1A1A2059236) and a grant from the Ministry of Health and welfare in Korea (Grant number, H112C-1210-010013).

## REFERENCES

- Dirks P, Bernstein M, Muller PJ, Tucker WS. The value of reoperation for recurrent glioblastoma. *Can J Surg J Can de Chir*. 1993;36(3):271–5.
- Gliniski B, Dymek P, Skolyszewski J. Altered therapy schedules in postoperative treatment of patients with malignant gliomas. Twenty year experience of the Maria Skłodowska-Curie Memorial Center in Krakow, 1973–1993. *J Neurooncol*. 1998;36(2):159–65.
- Legler JM, Ries LA, Smith MA, Warren JL, Heineman EF, Kaplan RS, *et al*. Cancer surveillance series [corrected]: brain and other central nervous system cancers: recent trends in incidence and mortality. *J Natl Cancer Inst*. 1999;91(16):1382–90.
- Tait MJ, Petrik V, Loosemore A, Bell BA, Papadopoulos MC. Survival of patients with glioblastoma multiforme has not improved between 1993 and 2004: analysis of 625 cases. *Br J Neurosurg*. 2007;21(5):496–500.
- Culver KW, Ram Z, Wallbridge S, Ishii H, Oldfield EH, Blaese RM. *In vivo* gene transfer with retroviral vector-producer cells for treatment of experimental brain tumors. *Science*. 1992;256(5063):1550–2.
- Klatzmann D, Valery CA, Bensimon G, Marro B, Boyer O, Mokhtari K, *et al*. A phase I/II study of herpes simplex virus type 1 thymidine kinase “suicide” gene therapy for recurrent glioblastoma. Study Group on Gene Therapy for Glioblastoma. *Hum Gene Ther*. 1998;9(17):2595–604.
- Ram Z, Culver KW, Oshiro EM, Viola JJ, DeVroom HL, Otto E, *et al*. Therapy of malignant brain tumors by intratumoral implantation of retroviral vector-producing cells. *Nat Med*. 1997;3(12):1354–61.
- Rainov NG, Fels C, Droege JW, Schafer C, Kramm CM, Chou TC. Temozolomide enhances herpes simplex virus thymidine kinase/ganciclovir therapy of malignant glioma. *Cancer Gene Ther*. 2001;8(9):662–8.
- Candolfi M, Yagiz K, Wibowo M, Ahlzadeh GE, Puntel M, Ghiasi H, *et al*. Temozolomide does not impair gene therapy-mediated antitumor immunity in syngeneic brain tumor models. *Clin Cancer Res*. 2014;20(6):1555–65.
- Kato T, Natsume A, Toda H, Iwamizu H, Sugita T, Hachisu R, *et al*. Efficient delivery of liposome-mediated MGMT-siRNA reinforces the cytotoxicity of temozolomide in GBM-initiating cells. *Gene Ther*. 2010;17(11):1363–71.
- Yang ZZ, Li JQ, Wang ZZ, Dong DW, Qi XR. Tumor-targeting dual peptides-modified cationic liposomes for delivery of siRNA and docetaxel to gliomas. *Biomaterials*. 2014;35(19):5226–39.
- Goel A, Kunnumakkara AB, Aggarwal BB. Curcumin as “Curcumin”: from kitchen to clinic. *Biochem Pharmacol*. 2008;75(4):787–809.
- Kunnumakkara AB, Anand P, Aggarwal BB. Curcumin inhibits proliferation, invasion, angiogenesis and metastasis of different cancers through interaction with multiple cell signaling proteins. *Cancer Lett*. 2008;269(2):199–225.
- Zhuang W, Long L, Zheng B, Ji W, Yang N, Zhang Q, *et al*. Curcumin promotes differentiation of glioma-initiating cells by inducing autophagy. *Cancer Sci*. 2012;103(4):684–90.
- Khaw AK, Hande MP, Kalthur G, Hande MP. Curcumin inhibits telomerase and induces telomere shortening and apoptosis in brain tumour cells. *J Cell Biochem*. 2013;114(6):1257–70.
- Das RK, Kasoju N, Bora U. Encapsulation of curcumin in alginate-chitosan-pluronic composite nanoparticles for delivery to cancer cells. *Nano Nanotechnol Biol Med*. 2010;6(1):153–60.
- Sahu A, Bora U, Kasoju N, Goswami P. Synthesis of novel biodegradable and self-assembling methoxy poly(ethylene glycol)-palmitate nanocarrier for curcumin delivery to cancer cells. *Acta Biomater*. 2008;4(6):1752–61.
- Park JH, Kim HA, Park JH, Lee M. Amphiphilic peptide carrier for the combined delivery of curcumin and plasmid DNA into the lungs. *Biomaterials*. 2012;33(27):6542–50.
- Kim HA, Park JH, Yi N, Lee M. Delivery of Hypoxia and Glioma Dual-Specific Suicide Gene Using Dexamethasone Conjugated Polyethylenimine for Glioblastoma-Specific Gene Therapy. *Mol Pharm*. 2014;In press.
- Lee M, Nah JW, Kwon Y, Koh JJ, Ko KS, Kim SW. Water-soluble and low molecular weight chitosan-based plasmid DNA delivery. *Pharm Res*. 2001;18(4):427–31.
- Lemkine GF, Goula D, Becker N, Palcari L, Levi G, Demeneix BA. Optimisation of polyethylenimine-based gene delivery to mouse brain. *J Drug Target*. 1999;7(4):305–12.
- Dhandapani KM, Mahesh VB, Brann DW. Curcumin suppresses growth and chemoresistance of human glioblastoma cells via AP-1 and NFkappaB transcription factors. *J Neurochem*. 2007;102(2):522–38.
- Kang SK, Cha SH, Jeon HG. Curcumin-induced histone hypoacetylation enhances caspase-3-dependent glioma cell death and neurogenesis of neural progenitor cells. *Stem Cells Dev*. 2006;15(2):165–74.
- Lee J, Hyun H, Kim J, Ryu JH, Kim HA, Park JH, *et al*. Dexamethasone-loaded peptide micelles for delivery of the heme oxygenase-1 gene to ischemic brain. *J Control Release*. 2012;158:131–8.
- Das L, Vinayak M. Anti-carcinogenic action of curcumin by activation of antioxidant defence system and inhibition of NF-kappaB signalling in lymphoma-bearing mice. *Biosci Rep*. 2012;32(2):161–70.
- Das L, Vinayak M. Curcumin attenuates carcinogenesis by down regulating proinflammatory cytokine interleukin-1 (IL-1alpha and IL-1beta) via modulation of AP-1 and NF-IL6 in lymphoma bearing mice. *Int Immunopharmacol*. 2014;20(1):141–7.
- Das L, Vinayak M. Long-term effect of curcumin down-regulates expression of tumor necrosis factor-alpha and interleukin-6 via modulation of E26 transformation-specific protein and nuclear factor-kappaB transcription factors in livers of lymphoma bearing mice. *Leukemia & lymphoma*. 2014.